GLOBECOM 2024 - 2024 IEEE Global Communications Conference | 979-8-3503-5125-5/24/$31.00 ©2024 IEEE | DOI: 10.1109/GLOBECOM52923.2024.10901716

Beamforming Design for RIS-aided ISAC: Maximizing Weighted Sum of SCNR and SINR

Jinming Zhang and Chenhao Qi
School of Information Science and Engineering, Southeast University, Nanjing, China
Email: {jmzhang, qch}@seu.edu.cn

***Abstract*—In this paper, we propose a fractional programming (FP)-based alternating optimization scheme to jointly design the transceiver beamforming at the integrated sensing and communication (ISAC) base station (BS) and the passive beamforming at the reconfigurable intelligent surface (RIS) for the RIS-aided ISAC system. The weighted sum of the signal-to-clutter-and-noise-ratio at the radar receiver of the BS and the smallest signal-to-interference-plus-noise ratio among all the communication users is maximized under the hardware constraints. Since it is difficult to directly obtain a solution for this non-convex FP problem, it is divided into three sub-problems that are alternately solved. The two sub-problems optimizing the transceiving beamforming at the BS are transformed into typical convex quadratic constraint quadratic programming ones using quadratic transformation. The other sub-problem optimizing the RIS passive beamforming is transformed into a manifold optimization one using Dinkelbach transformation. Simulation results verify the effectiveness of the proposed scheme.**

***Index Terms*—Beamforming, integrated sensing and communication (ISAC), millimeter wave, reconfigurable intelligent surface (RIS).**

I. Introduction

Integrated sensing and communication (ISAC) provides a new paradigm where radar and communication systems share the same frequency and hardware resources to improve the communication and sensing performance [1]–[3]. In the ISAC system, sensing and communication are deeply coupled in many aspects such as the waveform, the spectrum, the hardware and the spatial beamforming design [4], [5].

The combination of ISAC and other technologies, such as internet of things [6], millimeter wave (mmWave) communications and reconfigurable intelligent surface (RIS), is necessary in order to achieve better performance. RIS is a planar array consisting of many reflecting elements whose phase shifts can be smartly controlled. The reflection pattern can be reconfigured to benefit the signal propagation [7]. In fact, RIS-aided radar target detection technology is also put forward by researchers to improve the detection accuracy [8], especially in the mmWave system [9]. Thus, it attracts lots of research interest in the RIS-aided ISAC systems.

Most recent works on the RIS-aided ISAC systems investigate the beamforming and waveform design for both the ISAC base station (BS) and the RIS based on different performance metrics and constraints. Some works maximize the radar receiving signal-to-noise-ratio (SNR) under the constraints of the hardware facility and the communication performance. In fact, performance metrics such as Cramer-Rao bound of radar estimation and the mutual information for sensing, can also be exploited in transceiver beamforming and RIS passive beamforming design [10]. An alternative direction method of multipliers based algorithm is proposed to jointly design the transmit waveform and beamforming, to maximize the receiving signal-to-interference-plus-noise ratio (SINR) of the radar while satisfying the quality of service of wireless communications [11].

Note that the clutter patches typically exist together with the target, which causes the interference to the radar receiver. Consequently, the signal-to-clutter-and-noise-ratio (SCNR) is viewed as a crucial radar performance metric for target detection [12]. Thus, it is interesting to investigate the joint beamforming of the BS and RIS to achieve good SCNR performance and communication performance, which inspires our studies in this paper.

In this paper, we propose a fractional programming (FP)-based alternating optimization (AO) scheme to jointly design the transceiver beamforming at the BS and the passive beamforming at the RIS for the RIS-aided mmWave ISAC system. The weighted sum of the SCNR at the radar receiver and the smallest SINR among all the communication user equipment (UE) is maximized under the hardware constraints. Since it is difficult to directly obtain a solution for this non-convex FP problem, it is divided into three sub-problems that are alternately solved. The two sub-problems optimizing the transceiving beamforming at the BS are transformed into typical convex quadratic constraint quadratic programming (QCQP) ones using quadratic transformation. The other sub-problem optimizing the RIS passive beamforming is transformed into a manifold optimization one using Dinkelbach transformation.

We use the following notations in our paper. Symbols for vectors (lower case) and matrices (upper case) are in boldface. $(\cdot)^{\mathrm{T}}$, $(\cdot)^*$ and $(\cdot)^{\mathrm{H}}$ denote the transpose, conjugate and conjugate transpose (Hermitian), respectively. The set of $p \times q$ complex-valued matrices is denoted by $\mathbb{C}^{p\times q}$. $\|\boldsymbol{A}\|_{\mathrm{F}}$, $\|\boldsymbol{a}\|_2$ and $|a|$ denote the Frobenius norm of a matrix $\boldsymbol{A}$, the ℓ_2-norm of a vector $\boldsymbol{a}$ and the absolute value of a variable a. $[\boldsymbol{A}]_{i,j}$ represents the element on the ith row and jth column of $\boldsymbol{A}$. The complex Gaussian distribution is denoted by $\mathcal{CN}$. $\boldsymbol{I}_n$ is the n-dimensional identity matrix. We use $\mathrm{diag}\{\boldsymbol{a}\}$ to denote a square diagonal matrix with the elements of $\boldsymbol{a}$ on the main diagonal. $\mathrm{vec}\{\boldsymbol{A}\}$ means the vectorization of $\boldsymbol{A}$.

II. System Model

As shown in Fig. 1, a RIS-aided mmWave ISAC system includes a BS, a RIS, K single-antenna communication UEs, and a target. The RIS is connected to the BS via a wired link so that the BS can change the parameters of the RIS in real time. The RIS is equipped with N_{r} reflecting elements, which can passively reflect the incident signal. Each element of the RIS, which functions as a phase shifter for the incident signal, is independently controlled by the BS.

The BS is equipped with a uniform linear array (ULA) having N_{t} antennas and N_{R} radio frequency (RF) chains to simultaneously serve communication UEs and detect the target. The number of reflecting elements at the RIS is N_{r}. The transmit beamforming matrix of the BS can be written as

$$\boldsymbol{F} = [\boldsymbol{f}_1, \boldsymbol{f}_2, \cdots, \boldsymbol{f}_K, \boldsymbol{F}_{\mathrm{s}}], \tag{1}$$

where $\boldsymbol{f}_k \in \mathbb{C}^{N_{\mathrm{t}}}, k = 1, 2, \cdots, K$, represents the beamforming vector to transmit the communication signal to the kth user and $\boldsymbol{F}_{\mathrm{s}} \in \mathbb{C}^{N_{\mathrm{t}} \times (N_{\mathrm{R}} - K)}$ represents the beamforming matrix to transmit sensing signal to detect the target.

The radar receiver at the BS is equipped with a single RF chain and a ULA with N_{t} antennas. We use $\boldsymbol{w} \in \mathbb{C}^{N_{\mathrm{t}}}$ to denote the beamforming vector of the receiving ULA. The self interference can be eliminated with hardware isolation [12]. It is typically assumed that the channel between the BS and the RIS only contains a line-of-sight (LoS) path expressed as

$$\boldsymbol{H} = g\boldsymbol{\alpha}(N_{\mathrm{r}}, \phi_1)\boldsymbol{\alpha}^{\mathrm{H}}(N_{\mathrm{t}}, \phi_2), \tag{2}$$

where $g \sim \mathcal{CN}(0, 1)$, ϕ_1 and ϕ_2 represent the channel gain, the angle of departure (AoD) at the BS and the angle of arrival (AoA) at the RIS, respectively. The channel steering vector $\boldsymbol{\alpha}(N, \theta)$ as a function of N and θ is defined as

$$\boldsymbol{\alpha}(N, \theta) \triangleq \frac{1}{\sqrt{N}}[1, e^{j\pi\cos(\theta)}, e^{j\pi 2\cos(\theta)}, \cdots, e^{j\pi(N-1)\cos(\theta)}]^{\mathrm{T}}, \tag{3}$$

where N represents the number of antennas and θ represents the AoD or the AoA.

A. Communication Model

For wireless communications, we consider the downlink channel where the BS-UE LoS path and the BS-RIS-UE path both exist. We denote the channel between the RIS and the kth UE as $\boldsymbol{h}_k$ and the channel between the BS and the kth UE as $\boldsymbol{u}_k$, which can be written as

$$\begin{aligned} \boldsymbol{h}_k &= \xi_k \boldsymbol{\alpha}(N_{\mathrm{r}}, \theta_k), \\ \boldsymbol{u}_k &= e_k \boldsymbol{\alpha}(N_{\mathrm{t}}, \alpha_k). \end{aligned} \tag{4}$$

Here $\xi_k \sim \mathcal{CN}(0, 1)$, $e_k \sim \mathcal{CN}(0, 1)$, α_k, and θ_k represent the channel gain of the RIS-UE LoS path, the channel gain of the BS-UE LoS path, the AoA of the BS-UE LoS path, and the AoA of the RIS-UE LoS path for the kth UE, respectively.

We use the SINR of each user to evaluate the communication performance. The SINR of the kth user can be written as

$$\mathrm{SINR}_k = \frac{|\boldsymbol{c}_k^{\mathrm{H}} \boldsymbol{f}_k|^2}{\sum_{i=1, i\neq k}^{K} |\boldsymbol{c}_k^{\mathrm{H}} \boldsymbol{f}_i|^2 + \|\boldsymbol{c}_k^{\mathrm{H}} \boldsymbol{F}_{\mathrm{s}}\|_2^2 + \sigma_{\mathrm{c}}^2}, \tag{5}$$

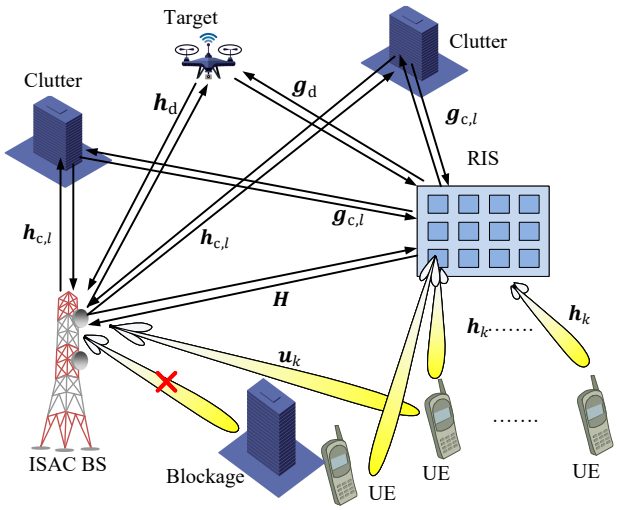

Fig. 1. Illustration of the RIS-aided mmWave ISAC system.

where the equivalent communication channel of the kth user is $\boldsymbol{c}_k^{\mathrm{H}} \triangleq (\boldsymbol{u}_k^{\mathrm{H}} + \boldsymbol{h}_k^{\mathrm{H}} \boldsymbol{V} \boldsymbol{H})$, the diagonal matrix $\boldsymbol{V} = \mathrm{diag}\{\boldsymbol{v}\}$ represents the passive beamforming of the RIS, and σ_{c}^2 is the variance of the complex Gaussian noise. We define

$$\boldsymbol{v} \triangleq [e^{jv_1}, e^{jv_2}, \cdots, e^{jv_{N_{\mathrm{r}}}}]^{\mathrm{T}}, \tag{6}$$

where $v_i, i = 1, 2, \cdots, N_{\mathrm{r}}$, is the phase shifts generated by the ith reflecting element of the RIS.

B. Target Sensing Model

For target sensing, the LoS path of BS-target can be expressed as

$$\boldsymbol{h}_{\mathrm{d}} = b_{\mathrm{d}} \boldsymbol{\alpha}(N_{\mathrm{t}}, \beta_{\mathrm{d}}), \tag{7}$$

where b_{d} and β_{d} represent the channel gain and the AoD of the LoS path, respectively. We suppose there are L clutter patches contributing to L channel paths in the sensing area. The channel contributed by the lth clutter patch can be expressed as

$$\boldsymbol{h}_{\mathrm{c},l} = b_l \boldsymbol{\alpha}(N_{\mathrm{t}}, \beta_l), \tag{8}$$

where b_l and β_l represent the channel gain and the AoD corresponding to the lth clutter patch, respectively.

Similarly, the LoS path of RIS-target and the LoS path between the RIS and the lth clutter patch can be written respectively as

$$\begin{aligned} \boldsymbol{g}_{\mathrm{d}} &= \kappa_{\mathrm{d}} \boldsymbol{\alpha}(N_{\mathrm{r}}, \gamma_{\mathrm{d}}), \\ \boldsymbol{g}_{\mathrm{c},l} &= \kappa_l \boldsymbol{\alpha}(N_{\mathrm{r}}, \gamma_l), \end{aligned} \tag{9}$$

where κ_{d} and κ_l represent the channel gain of $\boldsymbol{g}_{\mathrm{d}}$ and $\boldsymbol{g}_{\mathrm{c}}$, respectively, and γ_{d} and γ_l represent the AoD of $\boldsymbol{g}_{\mathrm{d}}$ and $\boldsymbol{g}_{\mathrm{c}}$, respectively.

Due to the channel reciprocity, the round-trip channel for target sensing can be expressed as

$$\boldsymbol{H}_{\mathrm{s}} = (\boldsymbol{h}_{\mathrm{d}} + \boldsymbol{H}^{\mathrm{H}} \boldsymbol{V}^{\mathrm{H}} \boldsymbol{g}_{\mathrm{d}})(\boldsymbol{h}_{\mathrm{d}}^{\mathrm{H}} + \boldsymbol{g}_{\mathrm{d}}^{\mathrm{H}} \boldsymbol{V} \boldsymbol{H}). \tag{11}$$

$$\begin{aligned} \max_{\boldsymbol{F}} \quad & \Bigg(\mu_1 \frac{\|\boldsymbol{w}^{\mathrm{H}}\boldsymbol{H}_{\mathrm{s}}\boldsymbol{F}\|_2^2}{\sum_{l=1}^{L}\|\boldsymbol{w}^{\mathrm{H}}\boldsymbol{G}_{\mathrm{s},l}\boldsymbol{F}\|_2^2} + \underbrace{\mu_2 \min_k \frac{|\boldsymbol{c}_k^{\mathrm{H}}\boldsymbol{f}_k|^2}{\sum_{i=1,i\neq k}^{K}|\boldsymbol{c}_k^{\mathrm{H}}\boldsymbol{f}_i|^2 + \|\boldsymbol{c}_k^{\mathrm{H}}\boldsymbol{F}_{\mathrm{s}}\|_2^2}}_{\mathrm{SINR-related\ terms}}\Bigg), \\ \text{s.t.} \quad & \|\boldsymbol{F}\|_{\mathrm{F}}^2 \le P_{\mathrm{T}}. \end{aligned} \tag{10}$$

Similarly, the round-trip channel corresponding to the lth clutter patch can be expressed as

$$\boldsymbol{G}_{\mathrm{s},l} = (\boldsymbol{h}_{\mathrm{c},l} + \boldsymbol{H}^{\mathrm{H}}\boldsymbol{V}^{\mathrm{H}}\boldsymbol{g}_{\mathrm{c},l})(\boldsymbol{h}_{\mathrm{c},l}^{\mathrm{H}} + \boldsymbol{g}_{\mathrm{c},l}^{\mathrm{H}}\boldsymbol{V}\boldsymbol{H}). \tag{12}$$

Since the SCNR is an important metric closely related to the detection probability and distance estimation of the target, we can express the SCNR as

$$\mathrm{SCNR} = \frac{\|\boldsymbol{w}^{\mathrm{H}}\boldsymbol{H}_{\mathrm{s}}\boldsymbol{F}\|_2^2}{\sum_{l=1}^{L}\|\boldsymbol{w}^{\mathrm{H}}\boldsymbol{G}_{\mathrm{s},l}\boldsymbol{F}\|_2^2 + \sigma_{\mathrm{s}}^2}, \tag{13}$$

where σ_{s}^2 is the variance of the complex Gaussian noise. Since the communication signal passing through K RF chains can also be used for target sensing, all the RF chains are involved in the computation of the SCNR.

III. FP-based AO Beamforming Scheme

In this section, we design the transceiver beamforming of the BS and the passive beamforming of the RIS for the RIS-aided mmWave ISAC system. Our objective is to maximize the weighted sum of the SCNR for sensing and the lowest SINR among all K UEs under the hardware constraints. The optimization problem can be written as

$$\begin{aligned} \max_{\boldsymbol{w},\boldsymbol{F},\boldsymbol{v}} \quad & \big(\mu_1 \mathrm{SCNR} + \mu_2 \min_k \mathrm{SINR}_{\mathrm{k}}\big), \\ \text{s.t.} \quad & \|\boldsymbol{F}\|_{\mathrm{F}}^2 \le P_{\mathrm{T}}, \\ & \|\boldsymbol{w}\|_2^2 \le 1, \\ & |[\boldsymbol{v}]_i| = 1, i = 1, 2, \cdots, N_{\mathrm{r}}, \end{aligned} \tag{14}$$

where μ_1 and μ_2 are two weighting coefficients for the trade-off between the sensing and communication performance, and P_{T} represents the transmit power of the BS.

This problem is a multi-ratio FP problem including the maximization of the minimum value, where obtaining a closed-form solution is difficult. In [13], different forms of FP problems in communications are investigated. The quadratic transformation can handle the fractional objective function with the non-convex quadratic numerator. In addition, to deal with the muti-variable FP, the existing works usually introduce the AO [12]. Therefore, we first exploit AO to divide (14) into three FP sub-problems and then solve them respectively.

A. Receive Beamforming Design

Given $\boldsymbol{F}$ and $\boldsymbol{v}$, the optimization of $\boldsymbol{w}$ can be written as

$$\begin{aligned} \max_{\boldsymbol{w}} \quad & \frac{\|\boldsymbol{w}^{\mathrm{H}}\boldsymbol{H}_{\mathrm{s}}\boldsymbol{F}\|_2^2}{\sum_{l=1}^{L}\|\boldsymbol{w}^{\mathrm{H}}\boldsymbol{G}_{\mathrm{s},l}\boldsymbol{F}\|_2^2}, \\ \text{s.t.} \quad & \|\boldsymbol{w}\|_2^2 \le 1, \end{aligned} \tag{15}$$

which is a single-ratio FP problem. Since the nominator and the denominator are both quadratic forms of $\boldsymbol{w}$, we use quadratic transformation to convert the problem into a convex one. Introducing an auxiliary vector $\boldsymbol{z} \in \mathbb{C}^{N_{\mathrm{R}}}$, (15) is equivalent to the following optimization problem as

$$\begin{aligned} \min_{\boldsymbol{w},\boldsymbol{z}} \quad & \big(\|\boldsymbol{z}\|^2\boldsymbol{w}^{\mathrm{H}}\boldsymbol{R}\boldsymbol{w} - 2\Re\{\boldsymbol{w}^{\mathrm{H}}\boldsymbol{H}_{\mathrm{s}}\boldsymbol{F}\boldsymbol{z}\}\big), \\ \text{s.t.} \quad & \|\boldsymbol{w}\|_2^2 \le 1, \end{aligned} \tag{16}$$

where $\boldsymbol{R} = \sum_{l=1}^{L}\boldsymbol{G}_{\mathrm{s},l}\boldsymbol{F}\boldsymbol{F}^{\mathrm{H}}\boldsymbol{G}_{\mathrm{s},l}^{\mathrm{H}}$. Fixing $\boldsymbol{z}$, the optimization of $\boldsymbol{w}$ is a typical convex QCQP optimization problem, which can be solved by the existing toolbox such as CVX. On the other hand, fixing $\boldsymbol{w}$, $\boldsymbol{z}$ can be updated by

$$\boldsymbol{z} = \boldsymbol{F}^{\mathrm{H}}\boldsymbol{H}_{\mathrm{s}}^{\mathrm{H}}\boldsymbol{w}. \tag{17}$$

Then we use AO to alternately optimize $\boldsymbol{z}$ and $\boldsymbol{w}$ with I_1 iterations. I_1 should be large enough to guarantee the convergence.

B. Transmit Beamforming Design

Given $\boldsymbol{w}$ and $\boldsymbol{v}$, the optimization of $\boldsymbol{F}$ can be written as (10). This is a multi-ratio max-min FP problem. Define $\boldsymbol{f} \triangleq \mathrm{vec}\{\boldsymbol{F}\}$. The nominator and the denominator are both quadratic forms of $\boldsymbol{f}$. Thus, we use quadratic transformation to convert (10) into a QCQP problem. For the max-min problem, we transform the SINR-related terms into K constraints with K auxiliary variables.

Such transformation dynamically searches for the maximum value of the minimum SINR among all the UEs, which makes it difficult to rigidly use μ_1 and μ_2. Thus, in this subproblem, we define a variable p to approximately represent the trade-off between sensing and communications. Note that we will rigidly use μ_1 and μ_2 in the next subsection for the optimization of $\boldsymbol{v}$ to ensure (14).

Define the auxiliary matrices $\boldsymbol{A}_k$, $\boldsymbol{A}$ and $\boldsymbol{D}$ as

$$\begin{aligned} \boldsymbol{A}_k &\triangleq [\underbrace{\boldsymbol{0},\cdots\boldsymbol{0}}_{k-1}, \boldsymbol{I}_{N_{\mathrm{t}}}, \underbrace{\boldsymbol{0},\cdots\boldsymbol{0}}_{N_{\mathrm{R}}-k}], \\ \boldsymbol{A} &\triangleq [\underbrace{\boldsymbol{I}_{N_{\mathrm{t}}},\cdots,\boldsymbol{I}_{N_{\mathrm{t}}}}_{N_{\mathrm{R}}}], \\ \boldsymbol{D} &\triangleq [\underbrace{\boldsymbol{0},\cdots,\boldsymbol{0}}_{K}, \underbrace{\boldsymbol{I}_{N_{\mathrm{t}}},\cdots,\boldsymbol{I}_{N_{\mathrm{t}}}}_{N_{\mathrm{R-K}}}]. \end{aligned} \tag{18}$$

With quadratic transformation and the auxiliary variables, we transform (10) into the following optimization problem as

$$\begin{aligned} \min_{\boldsymbol{f}} \quad & \big(|b|^2\boldsymbol{f}^{\mathrm{H}}\boldsymbol{T}\boldsymbol{f} - 2\Re\{b\boldsymbol{w}^{\mathrm{H}}\boldsymbol{H}_{\mathrm{s}}\boldsymbol{A}\boldsymbol{f}\}\big), \\ \text{s.t.} \quad & \|\boldsymbol{f}\|_2^2 \le P_{\mathrm{T}}, \\ & 2\Re\{b_k\boldsymbol{c}_k^{\mathrm{H}}\boldsymbol{A}_k\boldsymbol{f}\} - |b_k|^2(\boldsymbol{f}^{\mathrm{H}}\boldsymbol{Q}_k\boldsymbol{f}) - t_0 \ge 0, \\ & k = 1, 2, \cdots, K. \end{aligned} \tag{21}$$

$$\begin{aligned}\max_{\boldsymbol{v}} \quad & \left(\mu_1 \frac{\|\boldsymbol{w}^{\mathrm{H}}\boldsymbol{H}_{\mathrm{s}}(\boldsymbol{v})\boldsymbol{F}\|_2^2}{\sum_{l=1}^{L}\|\boldsymbol{w}^{\mathrm{H}}\boldsymbol{G}_{\mathrm{s},l}(\boldsymbol{v})\boldsymbol{F}\|_2^2} + \mu_2 \min_k \frac{|\boldsymbol{c}_k^{\mathrm{H}}(\boldsymbol{v})\boldsymbol{f}_k|^2}{\sum_{i=1,i\neq k}^{K}|\boldsymbol{c}_k^{\mathrm{H}}(\boldsymbol{v})\boldsymbol{f}_i|^2 + \|\boldsymbol{c}_k^{\mathrm{H}}(\boldsymbol{v})\boldsymbol{F}_{\mathrm{s}}\|_2^2}\right), \\ \text{s.t.} \quad & |[\boldsymbol{v}]_i| = 1, i = 1, 2, \cdots, N_{\mathrm{r}}.\end{aligned} \tag{19}$$

$$\begin{aligned}\max_{\boldsymbol{v}} \quad & \left(\mu_1\big(\|\boldsymbol{w}^{\mathrm{H}}\boldsymbol{H}_{\mathrm{s}}(\boldsymbol{v})\boldsymbol{F}\|_2^2 - t_1\sum_{l=1}^{L}\|\boldsymbol{w}^{\mathrm{H}}\boldsymbol{G}_{\mathrm{s},l}(\boldsymbol{v})\boldsymbol{F}\|_2^2\big) + \frac{\mu_2}{K}\big(\sum_{k=1}^{K}(|\boldsymbol{c}_k^{\mathrm{H}}(\boldsymbol{v})\boldsymbol{f}_k|^2 - t_2(\sum_{i=1,i\neq k}^{K}|\boldsymbol{c}_k^{\mathrm{H}}(\boldsymbol{v})\boldsymbol{f}_i|^2 + \|\boldsymbol{c}_k^{\mathrm{H}}(\boldsymbol{v})\boldsymbol{F}_{\mathrm{s}}\|_2^2))\big)\right), \\ \text{s.t.} \quad & |[\boldsymbol{v}]_i| = 1, i = 1, 2, \cdots, N_{\mathrm{r}}.\end{aligned} \tag{20}$$

In (21), b, t_0 and b_k are auxiliary variables and can be updated by

$$\begin{aligned} b &= \boldsymbol{f}^{\mathrm{H}}\boldsymbol{A}^{\mathrm{H}}\boldsymbol{H}_{\mathrm{s}}^{\mathrm{H}}\boldsymbol{w}, \\ b_k &= \boldsymbol{f}^{\mathrm{H}}\boldsymbol{A}_k^{\mathrm{H}}\boldsymbol{c}_k, \\ t_0 &= p\min_k \mathrm{SINR}_k, \end{aligned} \tag{22}$$

where SINR_k can be calculated by (5) in each iteration. Both $\boldsymbol{T}$ and $\boldsymbol{Q}_k$ are Hermitian matrices, and can be expressed respectively as

$$\begin{aligned} \boldsymbol{T} &= \textstyle\sum_{l=1}^{L}\boldsymbol{A}\boldsymbol{G}_{\mathrm{s},l}\boldsymbol{w}\boldsymbol{w}^{\mathrm{H}}\boldsymbol{G}_{\mathrm{s},l}^{\mathrm{H}}\boldsymbol{A}^{\mathrm{H}}, \\ \boldsymbol{Q}_k &= \textstyle\sum_{i=1,i\neq k}^{K}\boldsymbol{A}_i^{\mathrm{H}}\boldsymbol{c}_k\boldsymbol{c}_k^{\mathrm{H}}\boldsymbol{A}_i + \boldsymbol{D}^{\mathrm{H}}\boldsymbol{c}_k\boldsymbol{c}_k^{\mathrm{H}}\boldsymbol{D}. \end{aligned} \tag{23}$$

Fixing b, t_0 and b_k, (21) is a typical QCQP problem and can be solved by the existing toolbox. Similarly, we use AO to alternately optimize b, t_0, b_k and $\boldsymbol{f}$ with I_2 iterations.

C. RIS Passive Beamforming Design

Given $\boldsymbol{w}$ and $\boldsymbol{F}$, the optimization of $\boldsymbol{v}$ can be written as (19). This is a multi-ratio max-min FP problem with constant modulus constraints. The denominators and the nominators of the SCNR are quartic polynomials of $\boldsymbol{v}$. Here we use Dinkelbach transformation to deal with the fractional form. Introducing the auxiliary variables t_1 and t_2, (19) is equivalent to (20).

If (20) can be solved, then we can alternately update t_1 and t_2 respectively by

$$t_1 = \frac{\|\boldsymbol{w}^{\mathrm{H}}\boldsymbol{H}_{\mathrm{s}}(\boldsymbol{v})\boldsymbol{F}\|_2^2}{\sum_{l=1}^{L}\|\boldsymbol{w}^{\mathrm{H}}\boldsymbol{G}_{\mathrm{s},l}(\boldsymbol{v})\boldsymbol{F}\|_2^2}, \tag{24}$$

$$t_2 = \min_k \frac{|\boldsymbol{c}_k^{\mathrm{H}}\boldsymbol{f}_k|^2}{\sum_{i=1,i\neq k}^{K}|\boldsymbol{c}_k^{\mathrm{H}}\boldsymbol{f}_i|^2 + \|\boldsymbol{c}_k^{\mathrm{H}}\boldsymbol{F}_{\mathrm{s}}\|_2^2}. \tag{25}$$

In (20), the objective function and the constant modulus constraints are both non-convex. To deal with the non-convex constant modulus constraint, thirteen typical methods are summarized, such as semidefinite relaxation, unit projection and rank-one equivalent [14]. In this paper, we use the Riemannian manifold optimization to solve (20).

The feasible region of unit modulus constraint is known as complex circle manifold (CCM). The CCM optimization requires to calculate the gradient of the objective function in Euclidean space. Then it can be solved with the existing method [15]. Thus, we look into the objective function of $\boldsymbol{v}$ and its gradient in Euclidean space. In fact, the objective function in (20) consists of quartic polynomials of $\boldsymbol{v}$, which can be written as

$$\begin{aligned} L(\boldsymbol{v}) = {} & \mu_1\big(\boldsymbol{v}^{\mathrm{H}}\boldsymbol{B}_1\boldsymbol{v}\boldsymbol{v}^{\mathrm{T}}\boldsymbol{B}_2\boldsymbol{v}^* - t_1\textstyle\sum_{l=1}^{L}\boldsymbol{v}^{\mathrm{H}}\boldsymbol{B}_{1l}\boldsymbol{v}\boldsymbol{v}^{\mathrm{T}}\boldsymbol{B}_{2l}\boldsymbol{v}^*\big) \\ & +\mu_1\big(2\Re\{\boldsymbol{v}^{\mathrm{T}}\boldsymbol{k}\boldsymbol{v}^{\mathrm{H}}\boldsymbol{K}\boldsymbol{v}\} - t_1\textstyle\sum_{l=1}^{L}2\Re\{\boldsymbol{v}^{\mathrm{T}}\boldsymbol{k}_l\boldsymbol{v}^{\mathrm{H}}\boldsymbol{K}_l\boldsymbol{v}\}\big) \\ & +\mu_1\big(2\Re\{\boldsymbol{v}^{\mathrm{H}}\boldsymbol{x}\boldsymbol{v}^{\mathrm{H}}\boldsymbol{X}\boldsymbol{v}\} - t_1\textstyle\sum_{l=1}^{L}2\Re\{\boldsymbol{v}^{\mathrm{H}}\boldsymbol{x}_l\boldsymbol{v}^{\mathrm{H}}\boldsymbol{X}_l\boldsymbol{v}\}\big) \\ & +\boldsymbol{v}^{\mathrm{H}}\boldsymbol{M}_1\boldsymbol{v} + \boldsymbol{v}^{\mathrm{T}}\boldsymbol{M}_2\boldsymbol{v}^* + 2\Re\{\boldsymbol{v}^{\mathrm{H}}\boldsymbol{P}\boldsymbol{v}^*\} \\ & +2\Re\{\boldsymbol{q}_1\boldsymbol{v}\} + 2\Re\{\boldsymbol{q}_2\boldsymbol{v}^*\} + C. \end{aligned} \tag{26}$$

Here $\boldsymbol{B}_1$, $\boldsymbol{B}_2$, $\boldsymbol{B}_{1l}$, $\boldsymbol{B}_{2l}$, $\boldsymbol{k}$, $\boldsymbol{k}_l$, $\boldsymbol{K}$, $\boldsymbol{K}_l$, $\boldsymbol{x}$, $\boldsymbol{x}_l$, $\boldsymbol{X}$, $\boldsymbol{X}_l$, $\boldsymbol{M}_1$, $\boldsymbol{M}_2$, $\boldsymbol{P}$, $\boldsymbol{q}_1$, $\boldsymbol{q}_2$ and C are the coefficients of the quartic polynomial. They are the functions of all channel matrices, $\boldsymbol{w}$, $\boldsymbol{F}$ and μ_2. Due to the limitation of pages, their expressions are not shown here.

Then the gradient in the Euclidean space can be obtained via the differentiation of L, which can be written as

$$\begin{aligned} \boldsymbol{l}(\boldsymbol{v}) = {} & \mu_1\big(2\boldsymbol{v}^{\mathrm{T}}\boldsymbol{B}_2\boldsymbol{v}^*\boldsymbol{B}_1\boldsymbol{v} + 2\boldsymbol{v}^{\mathrm{H}}\boldsymbol{B}_1\boldsymbol{v}\boldsymbol{B}_2^{\mathrm{T}}\boldsymbol{v}\big) \\ & -t_1\mu_1\textstyle\sum_{l=1}^{L}\big(2\boldsymbol{v}^{\mathrm{T}}\boldsymbol{B}_{2l}\boldsymbol{v}^*\boldsymbol{B}_{1l}\boldsymbol{v} + 2\boldsymbol{v}^{\mathrm{H}}\boldsymbol{B}_{1l}\boldsymbol{v}\boldsymbol{B}_{2l}^{\mathrm{T}}\boldsymbol{v}\big) \\ & +2\mu_1\big(\boldsymbol{v}^{\mathrm{T}}\boldsymbol{k}\boldsymbol{K}\boldsymbol{v} + \boldsymbol{k}^{\mathrm{H}}\boldsymbol{v}^*\boldsymbol{K}^{\mathrm{H}}\boldsymbol{v} + \boldsymbol{v}^{\mathrm{H}}\boldsymbol{K}\boldsymbol{v}\boldsymbol{k}^*\big) \\ & -2t_1\mu_1\textstyle\sum_{l=1}^{L}\big(\boldsymbol{v}^{\mathrm{H}}\boldsymbol{K}_l\boldsymbol{v}\boldsymbol{k}_l + \boldsymbol{v}^{\mathrm{H}}\boldsymbol{k}_l\boldsymbol{K}_l\boldsymbol{v} + \boldsymbol{k}_l^{\mathrm{H}}\boldsymbol{v}\boldsymbol{K}_l^{\mathrm{H}}\boldsymbol{v}\big) \\ & +2\mu_1\big(\boldsymbol{v}^{\mathrm{H}}\boldsymbol{X}\boldsymbol{v}\boldsymbol{x} + \boldsymbol{v}^{\mathrm{H}}\boldsymbol{x}\boldsymbol{X}\boldsymbol{v} + \boldsymbol{x}^{\mathrm{H}}\boldsymbol{v}\boldsymbol{X}^{\mathrm{H}}\boldsymbol{v}\big) \\ & -2t_1\mu_1\textstyle\sum_{l=1}^{L}\big(\boldsymbol{v}^{\mathrm{H}}\boldsymbol{X}_l\boldsymbol{v}\boldsymbol{x}_l + \boldsymbol{v}^{\mathrm{H}}\boldsymbol{x}_l\boldsymbol{X}_l\boldsymbol{v} + \boldsymbol{x}_l^{\mathrm{H}}\boldsymbol{v}\boldsymbol{X}_l^{\mathrm{H}}\boldsymbol{v}\big) \\ & +2\boldsymbol{M}_1\boldsymbol{v} + 2\boldsymbol{M}_2^{\mathrm{T}}\boldsymbol{v} + 2(\boldsymbol{P} + \boldsymbol{P}^{\mathrm{T}})\boldsymbol{v}^* + 2\boldsymbol{q}_1^{\mathrm{H}} + 2\boldsymbol{q}_2^{\mathrm{T}}. \end{aligned} \tag{27}$$

Based on (26) and (27), (20) can be transformed into a standard CCM optimization problem, which can be solved by the existing toolbox [15]. Similarly, we use AO to alternately optimize t_1, t_2 and $\boldsymbol{v}$ with I_3 iterations.

Then we alternately solve the three subproblems until the objective function converges to a certain value. Note that both the SCNR and the minimum SINR can converge. For simplicity, here we set the stop condition of the AO iteration as

$$\frac{|\mathrm{SCNR}(t) - \mathrm{SCNR}(t-1)|}{\mathrm{SCNR}(t)} \leq \nu, \tag{28}$$

where t is the iteration index and ν is a small number. The complete steps of the FP-based AO beamforming scheme for the RIS-aided mmWave ISAC system can be summarized in **Algorithm 1**.

Algorithm 1 FP-based AO Scheme

Input: $\boldsymbol{H}$, $\boldsymbol{u}_k$, $\boldsymbol{h}_k$, $\boldsymbol{h}_{\mathrm{d}}$, $\boldsymbol{g}_{\mathrm{d}}$, $\boldsymbol{h}_{\mathrm{c},l}$, $\boldsymbol{g}_{\mathrm{c},l}$, I_1, I_2, I_3.
Initiation: Randomly select $\boldsymbol{f}$ and $\boldsymbol{v}$.
while (28) is not satisfied **do**
  Update i by $i \leftarrow i+1$.
  for $j = 1$ to I_1 **do**
    Obtain $\boldsymbol{w}_j$ by solving (16).
    Update $\boldsymbol{z}$ via (17).
  end for
  Update $\boldsymbol{w} \leftarrow \boldsymbol{w}_j$.
  Obtain $\boldsymbol{T}$ and $\boldsymbol{Q}_k$ via (23).
  for $j = 1$ to I_2 **do**
    Obtain $\boldsymbol{f}_j$ by solving (21).
    Update b, b_k and t_0 via (22).
  end for
  Obtain $L(\boldsymbol{v})$ and $\boldsymbol{l}(\boldsymbol{v})$ via (26) and (27), respectively.
  for $j = 1$ to I_3 **do**
    Obtain $\boldsymbol{v}$ by solving (20).
    Update t_1 and t_2 via (24) and (25), respectively.
  end for
  Update $\boldsymbol{H}_{\mathrm{s}}$, $\boldsymbol{G}_{\mathrm{s},l}$ via (11) and (12), respectively.
  Update $\boldsymbol{c}_k^{\mathrm{H}}$ by $\boldsymbol{c}_k^{\mathrm{H}} \leftarrow \boldsymbol{u}_k^{\mathrm{H}} + \boldsymbol{h}_k^{\mathrm{H}} \boldsymbol{V} \boldsymbol{H}$.
end while
Output: $\boldsymbol{v}$, $\boldsymbol{w}$, $\boldsymbol{F}$.

IV. Numerical Results

In this section, we evaluate the performance of the proposed scheme base on the given hardware resources.

Assume that there are $K = 3$ single-antenna UEs and one target in the RIS-aided mmWave ISAC system. The BS is equipped with a ULA consisting of $N_{\mathrm{t}} = 32$ antenna elements and $N_{\mathrm{R}} = 4$ RF chains. To sense the target, one dedicated RF chain is used, while three communication RF chains assist with their energy leakage. P_{T} is set to be $20\mathrm{dBW}$. The RIS is equipped with $N_{\mathrm{r}} = 32$ reflecting elements.

We assume that the locations of each UE and target are different in angular domain. The AoDs of the three BS-UE paths are $30°, 90°$ and $130°$. The AoDs of the three RIS-UE paths are $30°, 50°$ and $80°$. The AoDs of the BS-target and RIS-target paths are $60°$ and $115°$, respectively. For the channel between the BS and the RIS, the AoD and the AoA are set to be $45°$ and $90°$, respectively. We assume that the path loss of all communication paths is set the same to be $-90\mathrm{dB}$. The round-trip path loss of the BS-target and RIS-target paths is all set to be $-110\mathrm{dB}$. The receiving gains of the BS and the UEs are set to be $-40\mathrm{dB}$ and $-60\mathrm{dB}$, respectively. The variance of the Gaussian noise is assumed to be $\sigma_{\mathrm{c}}^2 = \sigma_{\mathrm{s}}^2 = -70\mathrm{dBm}$. Under such parameter settings, the SCNR and the SINR are at the comparable level and we set $\mu_1 = \mu_2 = 1$ in the simulations; otherwise, μ_1 or μ_2 should be multiplied by a factor in advance to ensure that the SCNR and SINR are at the comparable level.

First, we illustrate the relationship between the system performance and transmit power and the improvement brought by the RIS. For comparisons, the benchmark scheme uses the zero forcing (ZF) beamforming, while the RIS uses discrete Fourier transform (DFT) codewords.

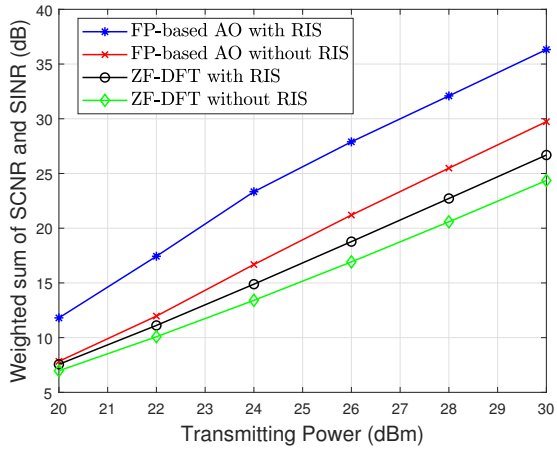

Fig. 2. Weighted sum of SCNR and SINR for different transmit power of the BS.

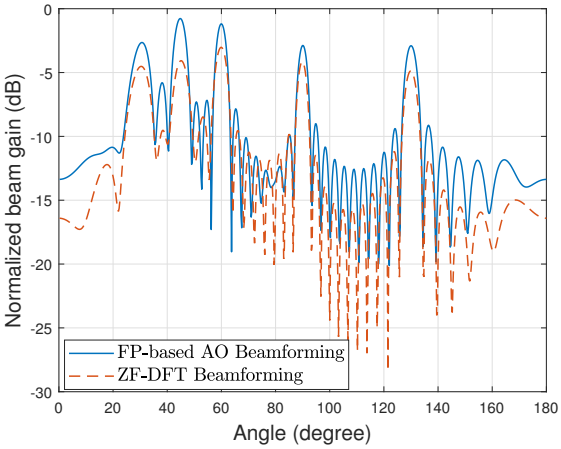

Fig. 3. Beam patterns of the BS with $\mu_1 = \mu_2 = 1$.

Fig. 2 illustrates the performance of the RIS-aided mmWave ISAC system shown by the weighted sum of SCNR and SINR versus the transmit power of the BS. Compared with the ZF-DFT scheme with RIS, FP-based AO beamforming scheme with RIS can achieve at least $9\mathrm{dB}$ performance improvement for the transmit power larger than $26\mathrm{dBm}$. Comparing the schemes with RIS to those without RIS, we can see that at least $6.6\mathrm{dB}$ improvement can be achieved by the FP-based AO beamforming scheme and $1.8\mathrm{dB}$ improvement by the ZF-DFT scheme.

Then we look into the beam patterns of the BS when $\mu_1 = \mu_2 = 1$. From Fig. 3, we can see that the BS exploit three BS-UE paths with three communication beams. The other two beams of the BS align with the BS-RIS and BS-target paths. In particular, the FP-based AO beamforming scheme not only reduces the mutual interference among different RF chains but also allocates the power to different paths based on the rigid

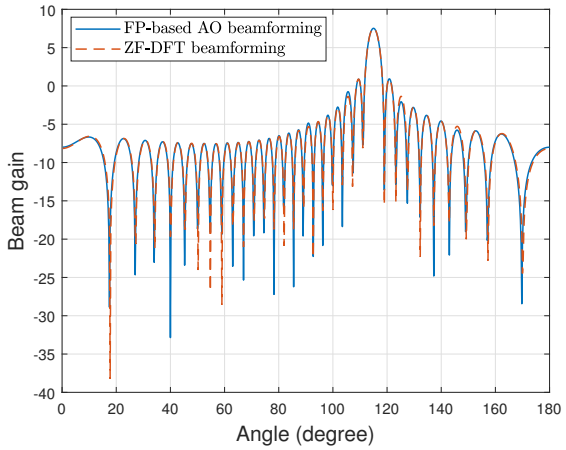

Fig. 4. Beam patterns at the RIS when the BS-UE LoS paths exist.

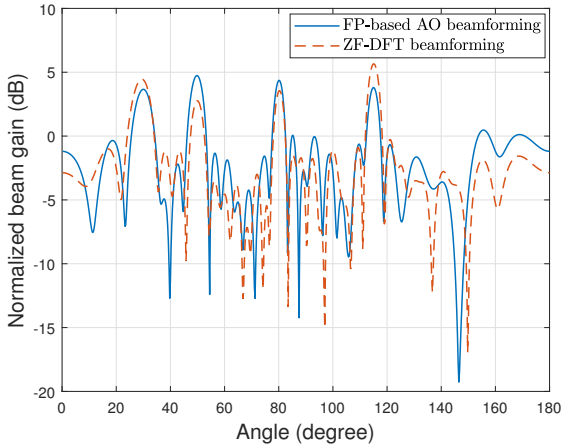

Fig. 5. Beam patterns of the RIS when the BS-UE LoS paths do not exist.

objective function. The mutual interference among different RF chains for the ZF-DFT scheme is larger than that of the FP-based AO scheme.

Fig. 4 compares the beam patterns of the RIS of two schemes. Since the BS-UE LoS paths exist, the BS allocates all the communication power to the beams aligned with the BS-UE LoS paths and does not use the BS-RIS path.

Then we look into the beam patterns at the RIS when the BS-UE LoS paths do not exist. Here the SINR is replaced with the SNR. In Fig. 5, we can see that three communication beams are aligned with the three BS-UE paths and one sensing beam is aligned with the BS-RIS-target path. Note that the power allocation of FP-based AO beamforming and ZF-DFT beamforming schemes is different. The FP-based AO beamforming scheme uses the rigid value obtained from the optimization, while the ZF-DFT beamforming scheme directly sets the weights of DFT codewords.

V. Conclusion

In this paper, we have proposed an FP-based AO beamforming scheme for the RIS-aided mmWave ISAC system to jointly design the transceiver beamforming at the BS and the passive beamforming at the RIS. The weighted sum of the SCNR and the smallest SINR among all UEs has been maximized under the hardware constraint. The optimization has been divided into three FP sub-problems that are alternately solved. Simulation results have verified the effectiveness of the proposed schemes. Future work will focus on the joint resource allocation for the RIS-aided mmWave ISAC system.

VI. Acknowledgment

This work is supported in part by National Natural Science Foundation of China (NSFC) under Grants U22B2007 and 62071116, and by National Key Research and Development Program of China under Grant 2021YFB2900404.

References

[1] F. Liu, C. Masouros, A. P. Petropulu *et al.*, "Joint radar and communication design: Applications, state-of-the-art, and the road ahead," *IEEE Trans. Commun.*, vol. 68, no. 6, pp. 3834–3862, June 2020.

[2] C. Qi, W. Ci, J. Zhang, and X. You, "Hybrid beamforming for millimeter wave MIMO integrated sensing and communications," *IEEE Commun. Lett.*, vol. 26, no. 5, pp. 1136–1140, May 2022.

[3] K. Chen and C. Qi, "Joint sparse Bayesian learning for channel estimation in ISAC," *IEEE Commun. Lett., early access*, pp. 1–5, 2024.

[4] J. A. Zhang, F. Liu, C. Masouros *et al.*, "An overview of signal processing techniques for joint communication and radar sensing," *IEEE J. Sel. Topics Signal Process.*, vol. 15, no. 6, pp. 1295–1315, Nov. 2021.

[5] K. Chen, C. Qi, O. A. Dobre, and G. Y. Li, "Simultaneous beam training and target sensing in ISAC systems with RIS," *IEEE Trans. Wireless Commun.*, vol. 23, no. 4, pp. 2696–2710, Apr. 2024.

[6] C. Qi, J. Wang, L. Lyu, L. Tan, J. Zhang, and G. Y. Li, "Key issues in wireless transmission for NTN-assisted internet of things," *IEEE Internet Things Mag.*, vol. 7, no. 1, pp. 40–46, Jan. 2024.

[7] Q. Wu, X. Zhou, W. Chen, J. Li, and X. Zhang, "IRS-aided WPCNs: A new optimization framework for dynamic IRS beamforming," *IEEE Trans. Wireless Commun.*, vol. 21, no. 7, pp. 4725–4739, July 2022.

[8] H. Zhang *et al.*, "Metaradar: Multi-target detection for reconfigurable intelligent surface aided radar systems," *IEEE Trans. Wireless Commun.*, vol. 21, no. 9, pp. 6994–7010, Sep. 2022.

[9] C. Qi, Q. Liu, X. Yu, and G. Y. Li, "Hybrid precoding for mixture use of phase shiftersand switches in mmWave massive MIMO," *IEEE Trans. Commun.*, vol. 70, no. 6, pp. 4121–4133, June 2022.

[10] N. Huang, T. Wang, Y. Wu, Q. Wu, and T. Q. S. Quek, "Integrated sensing and communication assisted mobile edge computing: An energy-efficient design via intelligent reflecting surface," *IEEE Wireless Commun. Lett.*, vol. 11, no. 10, pp. 2085–2089, Oct. 2022.

[11] R. Liu, M. Li, Y. Liu, Q. Wu, and Q. Liu, "Joint transmit waveform and passive beamforming design for RIS-aided DFRC systems," *IEEE J. Sel. Topics Signal Process.*, vol. 16, no. 5, pp. 995–1010, Aug. 2022.

[12] L. Xie, P. Wang, S. Song, and K. B. Letaief, "Perceptive mobile network with distributed target monitoring terminals: Leaking communication energy for sensing," *IEEE Trans. Wireless Commun.*, vol. 21, no. 12, pp. 10 193–10 207, Dec. 2022.

[13] K. Shen and W. Yu, "Fractional programming for communication systems-Part I: Power control and beamforming," *IEEE Trans. Signal Process.*, vol. 66, no. 10, pp. 2616–2630, May 2022.

[14] C. Pan *et al.*, "An overview of signal processing techniques for RIS/IRS-aided wireless systems," *IEEE J. Sel. Topics Signal Process.*, vol. 16, no. 5, pp. 883–917, Aug. 2022.

[15] P. A. Absil, R. Mahony, and R. Sepulchre, *Optimization algorithms on matrix manifolds*. Princeton University Press, 2009.